Heliyon 9 (2023) e21421

Contents lists available at ScienceDirect

Heliyon

journal homepage: www.cell.com/heliyon

Persulfate-assisted heterogeneous photocatalytic degradation of furfural from aqueous solutions using TiO_2–ZnO/biochar composite

Maryam Hasanzadeh [a], Zeinab Ghaedrahmat [b], Neda Kayedi [c], Neamatollah Jaafarzadeh Haghighi Fard [d,*], Ali Azari [e,**], Maryam Afsharizadeh [e]

[a] Student Research Committee, Department of Environmental Health Engineering, Ahvaz Jundishapur University of Medical Sciences, Ahvaz, Iran
[b] Department of Environmental Health Engineering, Shoushtar Faculty of Medical Sciences, Shoushtar, Iran
[c] Department of Environmental Health Engineering, School of Public Health, Jundishapour University of Medical Sciences, Ahvaz, Iran
[d] Environmental Technologies Research Center, Ahvaz Jundishapur University of Medical Sciences, Ahvaz, Iran
[e] Sirjan School of Medical Sciences, Sirjan, Iran

ARTICLE INFO

Keywords:
Furfural removal
TiO_2–ZnO/Biochar
Persulfate activation
Heterogeneous process
Photocatalytic degradation

ABSTRACT

This study evaluated the performance of TiO_2–ZnO/biochar as activator of persulfate (PS) for degradation of furfural. After the successful synthesis of the catalyst, X-ray diffraction (XRD), Fourier transform infrared spectroscopy (FTIR), and scanning electron microscopy (SEM) methods were used to investigate the properties of TiO_2–ZnO/biochar. The findings of this research suggests that under optimal conditions (pH = 3, catalyst dosage = 1 g/L, persulfate concentration = 1.2 mM, and furfural concentration = 10 mg/L), the PS/Catalysts/UV system can remove 96 % of furfural within 15 min. Under ideal conditions, the experimental results fit well with the first-order kinetic model ($R^2 > 0.95$), and the rate constant (K_{obs}) was derived as 0.195 min^{-1}. The quenching experiments provided further insights that confirmed the participation of $SO_4^{\circ -}$ and OH° radicals in the degradation process. Nevertheless, the evidence strongly supports the idea that $SO_4^{\circ -}$ plays a more prominent and dominant role as the primary radical species responsible for furfural degradation. Based on the obtained results, it can be concluded that the PS/Catalysts/UV system has an appropriate ability to remove furfural from aqueous solutions, which suggests promising perspectives for its practical application in pollutant treatment scenarios.

1. Introduction

Iran's oil and petrochemical industries are crucial, accounting for a significant portion of exports and GDP. However, these industries also contribute to environmental pollution, especially water resources [1]. The chemical compounds released by these industries are often complex and durable, toxic and non-degradable, making them a significant challenge for conventional wastewater treatment systems [2]. Furfural is an example of a pollutant produced by petrochemical industries in a significant amount and enters

* Corresponding author.
** Corresponding author.
E-mail addresses: n.jaafarzade@gmail.com, Jaafarzadeh-n@ajums.ac.ir (N.J. Haghighi Fard), azari.hjh@Gmail.com, a.azari@sirums.ac.ir (A. Azari).

https://doi.org/10.1016/j.heliyon.2023.e21421
Received 14 August 2023; Received in revised form 13 October 2023; Accepted 20 October 2023
Available online 21 October 2023

the ecosystem [3]. Researchers have reported lung, liver, kidney, spleen problems, and fuefural carcinogenicity. On the other hand, headaches, severe skin, eye, mucous irritation and pulmonary edema have also been observed after exposure to furfural [4,5]. As a result, removing furfural before discharging it into receiving resources is vital for both human and environmental health. Because of its better efficiency and possible benefits over conventional treatment methods, the advanced oxidation process (AOP) has gained attention as a promising technology for eliminating furfural and other organic contaminants from wastewater [6–8]. Advanced oxidation processes (AOPs) rely on the production of extremely reactive hydroxyl radicals (OH°), which may successfully oxidize and degrade furfural molecules into simpler and less toxic chemicals. Typically, oxidizing agents like hydrogen peroxide, ozone, or UV radiation are used in this process. These agents can be used alone or in combination with other oxidizing agents and catalysts to increase the production of hydroxyl radicals and increase the stability of the AOP process [9]. Sulfate radical-based advanced oxidation processes (S-AOPs) have a high redox potential and a long lifetime, making them attractive for removing several contaminants from wastewater [10]. The S-AOPs involve the generation of sulfate radicals ($SO_4^{\circ -}$), which are highly reactive and can effectively oxidize and degrade a wide range of organic pollutants. Different activation methods produce sulfate radicals from persulfate or peroxymonosulfate anions, including thermal processes, transition metal cations, ultrasound and ultraviolet irradiation and heterogeneous photocatalysts [11,12]. TiO_2 is a widely used photocatalyst due to its favorable physicochemical properties, high reactivity, cost-effectiveness, chemical stability and availability. However, TiO_2 has some limitations that make it less than ideal for certain photocatalytic applications [13,14]. One of the main limitations of TiO_2 is its tendency to recombine photoinduced charge carriers too quickly. This reduces the photocatalytic process efficiency. This is because the excited electrons and holes generated by light absorption in the TiO_2 tend to recombine before they can participate in chemical reactions with the target pollutants. This rapid recombination of charge carriers limits the lifetime of excited states, limiting photocatalytic process efficiency. Another limitation of TiO_2 is its limited ability to utilize visible light efficiently. TiO_2 absorbs ultraviolet (UV) light, which accounts for only a small portion of the solar spectrum. As a result, TiO_2-based photocatalysts can only be used in situations where UV light is the energy source [15,16]. Combining TiO_2 with ZnO has been studied extensively to enhance photocatalytic properties. The resulting composite materials have improved photocatalytic activity and stability, making them promising candidates for sulfate radical-based advanced oxidation processes (S-AOPs) to degrade pollutants in wastewater [14,17]. One of the advantages of combining TiO_2 with ZnO is the synergistic effect between the two materials. TiO_2 has high photocatalytic activity, but its performance is limited by its tendency to recombine photoinduced charge carriers quickly. On the other hand, ZnO has lower photocatalytic activity than TiO_2 but a longer lifetime of photoinduced charge carriers. Therefore, by combining TiO_2 with ZnO, the resulting composite can have improved photocatalytic properties, such as higher activity and better stability [18,19]. Another advantage of combining TiO_2 with ZnO is broadening the light harvesting range. TiO_2 absorbs UV light, while ZnO can absorb both UV and visible light. As a result, mixing TiO2 and ZnO can enhance photocatalytic activity when exposed to visible light, which is more abundant in the solar spectrum. According to some researchers, carbon-based materials have the good potential to enhance oxidation and breakdown of pollutants due to their favorable photoelectric properties. These properties include efficient electron transport and storage, which improves photoinduced charge separation efficiency. As a result, carbon-based materials, such as biochar, are being investigated as an effective and low-cost solution to addressing environmental pollution [20,21]. Hence, biochar was selected as a carbon-based material for this investigation due to numerous advantageous. These include its narrow band gap, which allows it to absorb light in the visible range and generate photoinduced charges for pollutant breakdown. Biochar is also easy to prepare using a simple pyrolysis process. It can be produced from various raw materials, making it a versatile option for pollutant removal.

Additionally, biochar is relatively cheap, making it an attractive choice for large-scale environmental applications [22]. Accordingly, it is anticipated that the combination of TiO2/ZnO and biochar will be able to modify the energy gap (Eg) of catalysts and increase the range of light harvesting, both of which would enhance the activation of persulfate and the performance of visible-light-driven photocatalysis. As a result, under UV light, the TiO2–ZnO/biochar nanocomposites may generate electrons in the conduction band that persulfate ions can consume to create sulfate anion radicals that are used to degrade furfural [23,24].

Considering the challenges highlighted, this study was undertaken to achieve the following objectives: (I) Synthesis of TiO_2–ZnO/biochar (TZB) nanocomposites and characterizing their morphology. (II) Assess the effectiveness of TZB in degrading furfural by investigating the influence of operating parameters such as pH, various initial concentrations, catalyst doses and PS concentration. (III) Investigate and establish the degradation kinetics of the TZB nanocomposites.

2. Experimental

2.1. Chemicals and instruments

Chemicals and reagents were analytical grade and used without additional purification. Sigma Aldrich (St. Louis, MO, USA) provided the zinc nitrate ($Zn(NO_3)_2$), tetrabutyl titanate ($Ti(C_4H_9O)_4$), acetic acid (CH_3COOH), sodium hydroxide (NaOH), methanol (CH_3OH), and hydrochloric acid (HCl). Merck Co. (Darmstadt, Germany) supplied the furfural ($C_5H_4O_2$). All of the standard solutions were made using distilled water. 1 N HCL and NaOH were used for adjusting the pH of the solution. A cubic magnet with a magnetic field of 3000 Gauss separated the solid phase from the solution.

2.2. Synthesis of catalysts and its characterization

Biochar was derived through the pyrolysis of reed straw feedstock under low oxygen conditions at 500 °C for a duration of 6 h. Subsequently, it was subjected to milling to achieve a particle size that passes through a 0.15 mm sieve. Following this, the biochar was

subjected to multiple rinses with ultrapure water (UPW) to maintain a neutral pH and then dried at 105 °C. The TiO_2–ZnO/biochar (TZB) nanocomposites were prepared using a sol-gel method originally described by Zhang [25], with some modifications. Specifically, 3g of $Zn(NO_3)_2$, 1g of biochar, and 25 mL of acetic acid were combined in 50 mL of ethanol and sonicated for 30 min. Then, 40 mL of tetrabutyl titanate, serving as the precursor, was added dropwise to the mixture while mechanically stirring for 2 h at room temperature. A volume of 25 mL of ultrapure water (UPW) with a pH of 2 was introduced into the solution with constant stirring for a duration of 4 h, resulting in the formation of a black sol. This sol was subsequently allowed to age for two days and was then subjected to drying at 105 °C for 8 h. Finally, the dried material underwent calcination at 300 °C for 2 h to yield the as-prepared TZB. The morphology and surface characteristics of the catalyst were analyzed using scanning electron microscopy (SEM), specifically a Hitachi S-4700 instrument based in Tokyo, Japan. To examine the phases and crystalline structure of the samples, X-ray diffraction analyses (XRD) were conducted using a D/MAX 2500 apparatus from Rigaku, USA, equipped with CuKα radiation at 40 kV and 40 mA, along with a positional sensitive detector (PSD) such as the Philips X-Cellerator. The chemical structure, including functional groups, of the synthesized catalyst was determined through Fourier transform infrared spectroscopy (FT-IR), employing a Nexus TM 670 instrument [26].

2.3. Degradation experiments

The degradation of furfural by TZB nanocomposites was carried out within a specially constructed reactor using varying concentrations of the pollutant. Prior to UV irradiation, a mechanical stirrer was employed to mix the furfural and catalyst for 30 min. This step aimed to establish adsorption-desorption equilibrium on the catalyst's surface and eliminate the impact of adsorption during the

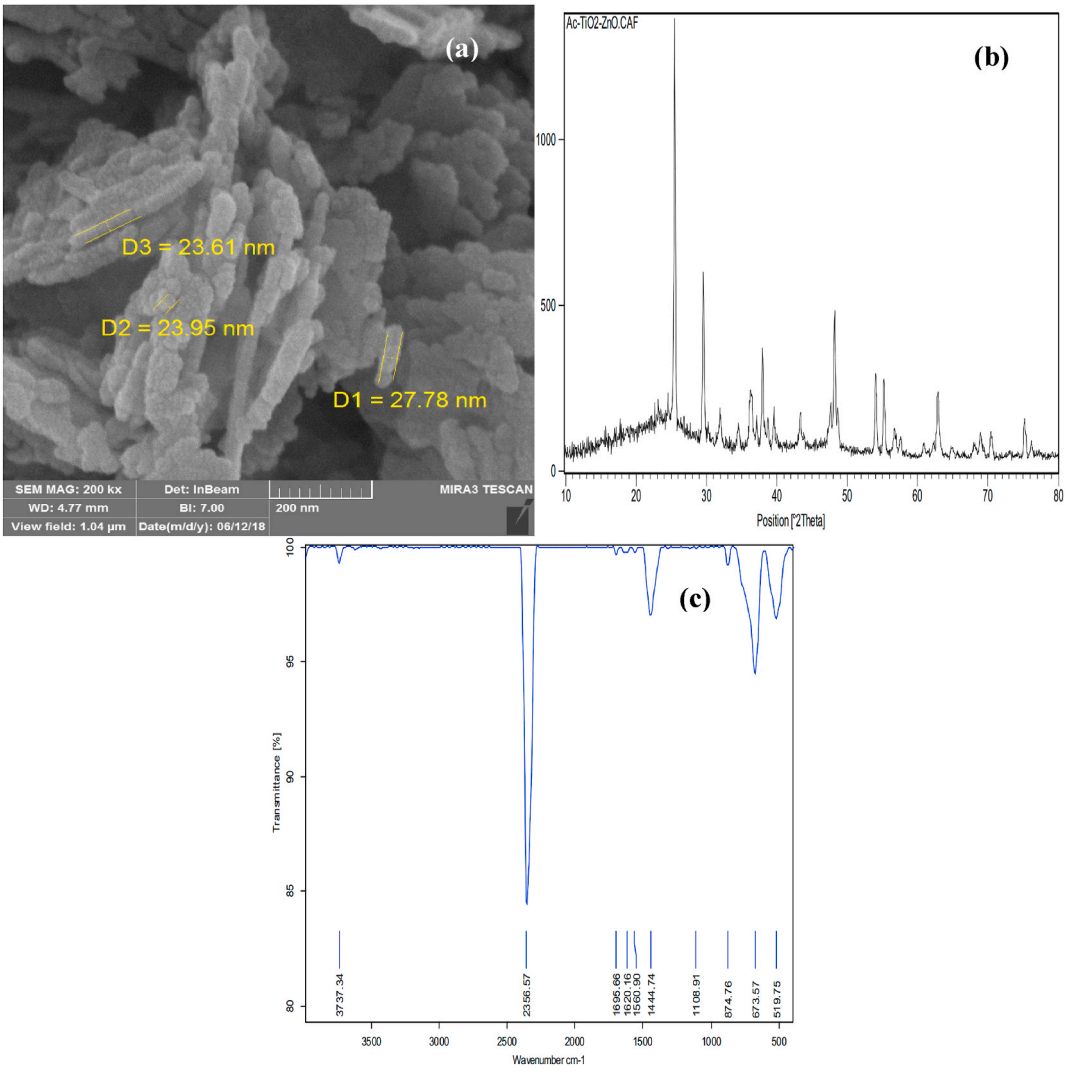

Fig: 1. SEM (a), XRD (b) and FTIR (c) of synthesized TZB.

photocatalytic degradation process. The investigation of the degradation process involved the assessment of key parameters, encompassing pH (ranging from 3 to 11), catalyst quantity (ranging from 0 to 1.5 g/L), persulfate concentration (varying from 0.4 to 1.2 mM), and initial concentration of furfural (ranging from 10 to 45 mg/L), with respect to contact time. The Eq. (1) was used to describe the ability of the TZB nanocomposites to degrade furfural:

$$\text{Degradation } \% = \left(\frac{C_0\text{-}C_e}{C_0}\right) \times 100 \quad (1)$$

Where C_0 and C_e represent the initial and residual concentrations of furfural (mg/L), respectively. The kinetics of the degradation process were also explored and reported. Given that first-order kinetics are commonly employed to describe the degradation of organic and inorganic pollutants [27], this study assessed the furfural degradation rate using a first-order kinetic equation (**Eq. (2)**):

$$\ln\left(\frac{C_0}{C_e}\right) = K_{obs} \times t \quad (2)$$

where K_{obs} denotes the rate of the reaction (min^{-1}), C_0 and C_e represent the initial and residual concentrations of contaminants (mg/L), and t stands for the time (min). It is important to note that all experiments were conducted in triplicate, and the average results were reported.

3. Results and discussion

3.1. Samples characterization

Fig. 1(a) displays scanning electron microscope (SEM) images of the synthesized TZB. It is evident from the images that the synthesized TZB exhibits a cylindrical and asymmetrical structure, with a size distribution falling within the range of 23–30 nm. Notably, the surface of the samples appears to be rough and porous, featuring a series of holes. This porous structure enhances the

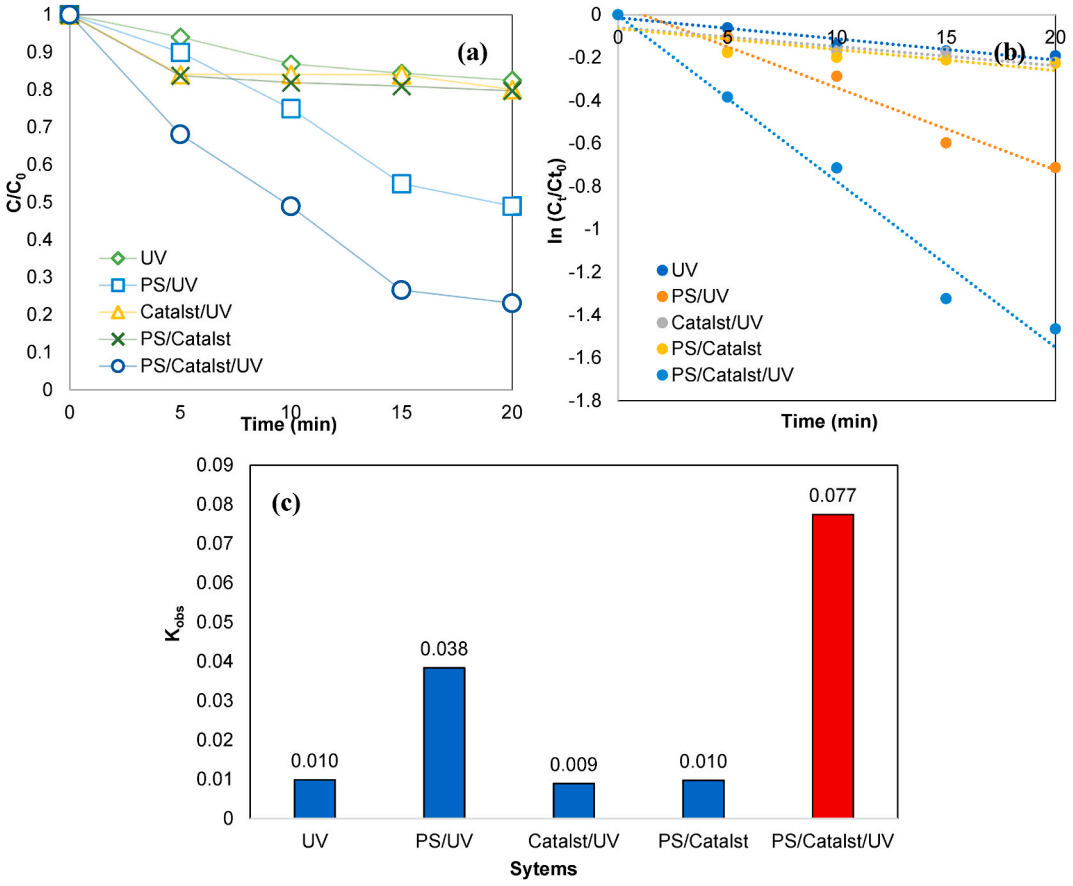

Fig: 2. Furfural degradation efficiency (a), investigation of the kinetic (b), and determination of the reaction rate constant (c) for experimental systems.

contact between furfural and TZB, thereby contributing to improved degradation performance. In Fig. 1(b), X-ray diffraction (XRD) patterns of the synthesized TZB within the 2θ range of 10–80° are presented for analysis. The diffraction peaks at 25.16° for (101), 37.82° for (004), 48.06° for (200), 55.17° for (211), 62.69° and 70.48° for (220) based on JCPDS No. 21–1272 indicate TiO_2 with an anatase tetragonal structure. The diffraction peaks at 2θ equal 31.77° (100) and 56.60° (110) according to JCPDS No. 36–1451 standard corresponding to ZnO. The above results confirm the successful synthesis of TiO_2–ZnO and its stabilization on biochar. In Fig. 1(c), Fourier-transform infrared spectroscopy (FTIR) of the synthesized TZB is presented within the spectral range of 4000–450 cm^{-1}. The FTIR analysis reveals several noteworthy features: The O–H (hydroxyl) group on the synthesized TZB is apparent as a broad band centered around 3737 cm^{-1}. A distinct band at 519.75 cm^{-1} corresponds to Ti–O vibration, signifying the presence of TiO2 within the material. The presence of a peak at 673 cm^{-1} is attributed to the Zn–O–Ti bond, providing confirmation of the presence of TiO_2–ZnO in the catalyst. Peaks at 1444 cm^{-1} and 2356 cm^{-1} are indicative of the C═O and N–O stretching vibrations, respectively.

3.2. Furfural degradation over various systems

Fig. 2 illustrates the efficiency of the PS/Catalysts/UV system in comparison to UV, PS/UV, Catalysts/UV, and PS/Catalysts processes under the following experimental conditions: PS concentration of 1 mM, catalyst dosage of 1 g/L, initial furfural concentration of 20 mg/L, and a total volume of 200 mL. According to Fig. 2(a), it can be found that after 15 min, furfural degradation efficiency shows an almost constant trend. Furfural removal efficiencies by UV were very low after 15 min (15.6 %), showing that furfural cannot be degraded enough by UV alone. Fig. 2(a) illustrates that furfural degradation efficiency remains relatively constant/stable after the first 15 min of the experiment. UV alone exhibits low furfural removal efficiency after 15 min, indicating that UV alone is not sufficient for substantial furfural degradation (15.6 %). In contrast, higher removal efficiencies are observed in PS/UV (45 %), Catalysts/UV (16 %), and PS/Catalysts (19.02 %) systems, highlighting the impact of these processes. Remarkably, when furfural is exposed to the PS/Catalysts/UV system, the removal efficiency experiences a significant increase, reaching 73.4 %. Fig. 2(b) demonstrates that the kinetic study of furfural degradation across various systems aligns well with the first-order kinetic model, with R^2 values exceeding 0.9. The degradation constant (K_{obs}) values were calculated for different systems, as illustrated in Fig. 2(c). In the PS/Catalysts/UV system, the rate constant for furfural removal is 0.077 min^{-1}, significantly higher than the values of 0.010, 0.038, 0.009, and 0.010 min^{-1} observed for UV, PS/UV, Catalysts/UV, and PS/Catalysts, respectively. These outcomes affirm that the incorporation of TiO_2 in the PS/

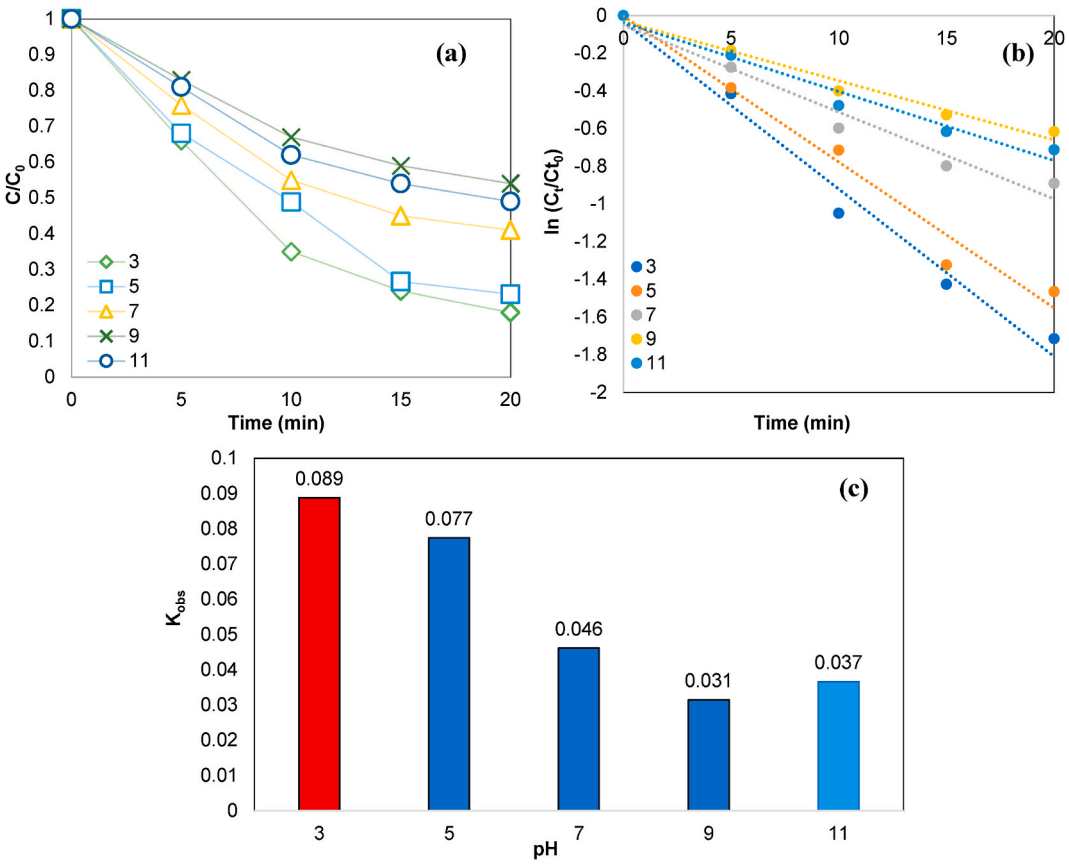

Fig. 3. Effect of pH on furfural degradation (PS: 1 mM, Catalysts dosage: 1 g/L, initial concentration: 20 mg/L, Volume: 200 mL) (a), kinetic study (b) and rate constant (c).

Catalysts/UV system plays a decisive role in considerably reducing furfural toxicity. This indicates the presence of a synergistic effect between the combined agents, demonstrating the potential of this process in furfural degradation and reduction of its environmental impact.

3.3. Effect of operational parameters and kinetic studies

3.3.1. Effect of pH

The pH of the solution influences furfural degradation efficiency using TZB nanocomposites. This is because the charged states of the catalyst, PS, and furfural molecules vary with pH. This affects the adsorption, activation, and reaction of these species on the catalyst surface. Hence, the impact of the initial pH of the solution (ranging from 3 to 11) on the removal efficiency of furfural in the PS/Catalysts/UV system was assessed (refer to Fig. 3(a)). In the first 15 min of the reaction, degradation efficiencies exhibited a decline of approximately 31 % as the pH levels were elevated from 3 to 11. It is noteworthy that acidic conditions are preferable for the degradation of furfural within the PS/Catalysts/UV systems. Simultaneously, the corresponding degradation rate constants (k_{obs}) for furfural decreased from 0.089 to 0.037 min^{-1} as the solution's pH increased from 3 to 11(Fig. 3(b-c)). The pKa values of furfural and PS (persulfate) are 9.5 and 9.4, respectively. When the pH increases to 9.5, more furfural molecules dissociate into ions, while PS is predominantly HSO_5^-. The synthesized catalyst has a point of zero charge (PZC) of 7.67. As a result, when pH levels surpass 7.67, the catalyst surface acquires a negative charge. Conversely, at pH values lower than 7.67, the catalyst surface takes on a positive charge. Therefore, with decreasing pH, furfural and PS experience a shift towards negative charge, thereby promoting their adsorption onto the positively charged surface of the catalyst. The catalyst surface can activate PS using electrons, generating sulfate radicals ($SO_4^{\circ-}$) that oxidize furfural adsorbed on the catalyst surface. Furthermore, furfural reacts with other free radicals and holes on the catalyst surface. However, when the pH of the furfural solution turns toward alkaline conditions (>9.5), the negative charge on the catalyst surface can create a repulsive force that reduces furfural degradation efficiency. Moreover, high concentrations of OH^- ions can quench the sulfate radicals ($SO_4^{\circ-}$), which have a shorter lifetime and lower selectivity than the SO° radical [28,29]. These factors can further decrease furfural removal efficiency. Therefore, it is crucial to control the pH of the solution to 3 to optimize TZB nanocomposites in furfural degradation performance.

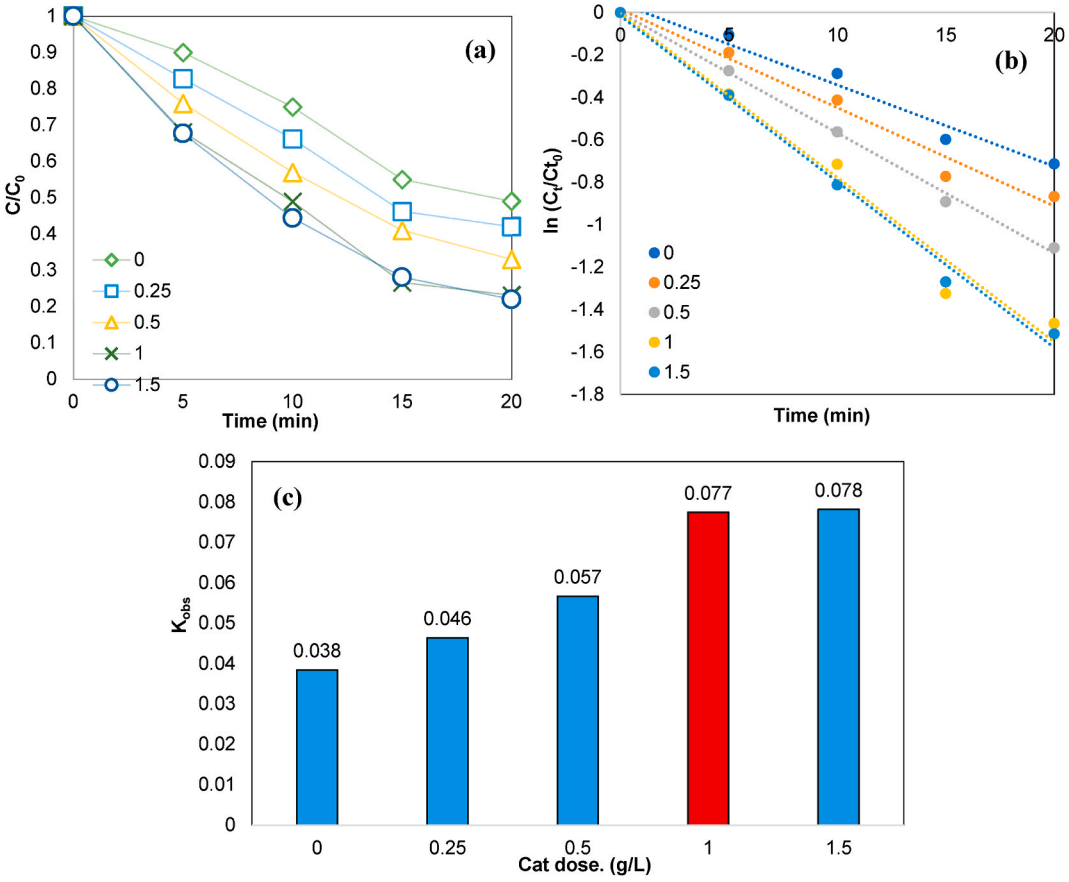

Fig. 4. Effect of catalyst dosage (g/L) on furfural degradation (PS: 1 mM, pH: 3, initial concentration: 20 mg/L, Volume: 200 mL) (a), kinetic study (b) and rate constant (c).

3.3.2. Effect of catalyst amount

In Fig. 4(a), the influence of varying quantities of TZB nanocomposites on the degradation of furfural is illustrated. Findings from Fig. 4(b-c) reveal that increasing the catalyst dosage from 0.25 g/L to 1 g/L results in an enhancement of the furfural degradation rate, ranging from 0.046 to 0.077 min^{-1}, and an increase in furfural degradation efficiency from 58 % to 76.9 %. The rise in the degradation rate and efficiency can be ascribed to the increased availability of additional electron-hole pairs [28,30]. With a higher dose of photocatalyst, more electron-hole pairs are generated, activating more PS and enhancing furfural degradation. However, it is important to note that the rate constant and removal efficiency do not improve beyond a TiO_2–ZnO/biochar dose of 1 g/L. This observation can be explained by the finite amount of PS available in the system, when added and produced by electron excitation [28]. As a result, there is a maximum achievable degradation efficiency for any given system, which cannot be exceeded even at higher catalyst doses. Based on the study results, the optimal photocatalyst dose was 1 g/L of catalyst.

3.3.3. Effect of the PS concentration

The impact of varying concentrations of persulfate (PS) on the efficacy of furfural degradation utilizing TZB nanocomposites was investigated under conditions of pH = 3 and a catalyst dose of 1 g/L over a 20-min duration. The outcomes are presented in Fig. 5(a-c). The data illustrates that increasing the PS concentration from 0.4 to 1.2 mM resulted in an extensive enhancement of degradation efficiency, with a 42 % increase and an augmented degradation rate (K_{obs}) of 82 %. The enhancement observed can be ascribed to the increased presence of $SO4^{\circ -}$ and OH° radicals generated through the activation of PS, which promote furfural breakdown [31–33]. Nonetheless, it was noted that increasing the PS concentration beyond 1 mM did not yield a significant improvement in degradation efficiency. This phenomenon could be attributed to the scavenging effect of persulfate at higher concentrations, as elucidated in **Eqs. (3) and (4)** [34]. The scavenging effect impedes the efficacy of persulfate radicals in the degradation process. Despite this limitation, the study identifies an optimal PS concentration of 1.2 mM, which enables superior furfural degradation.

$$SO_4^{\circ -} + S_2O_8^{2-} \rightarrow S_2O_8^{\circ -} + SO_4^{2-} \quad (3)$$

$$OH^{\circ} + S_2O_8^{2-} \rightarrow S_2O_8^{\circ -} + OH^{-} \quad (4)$$

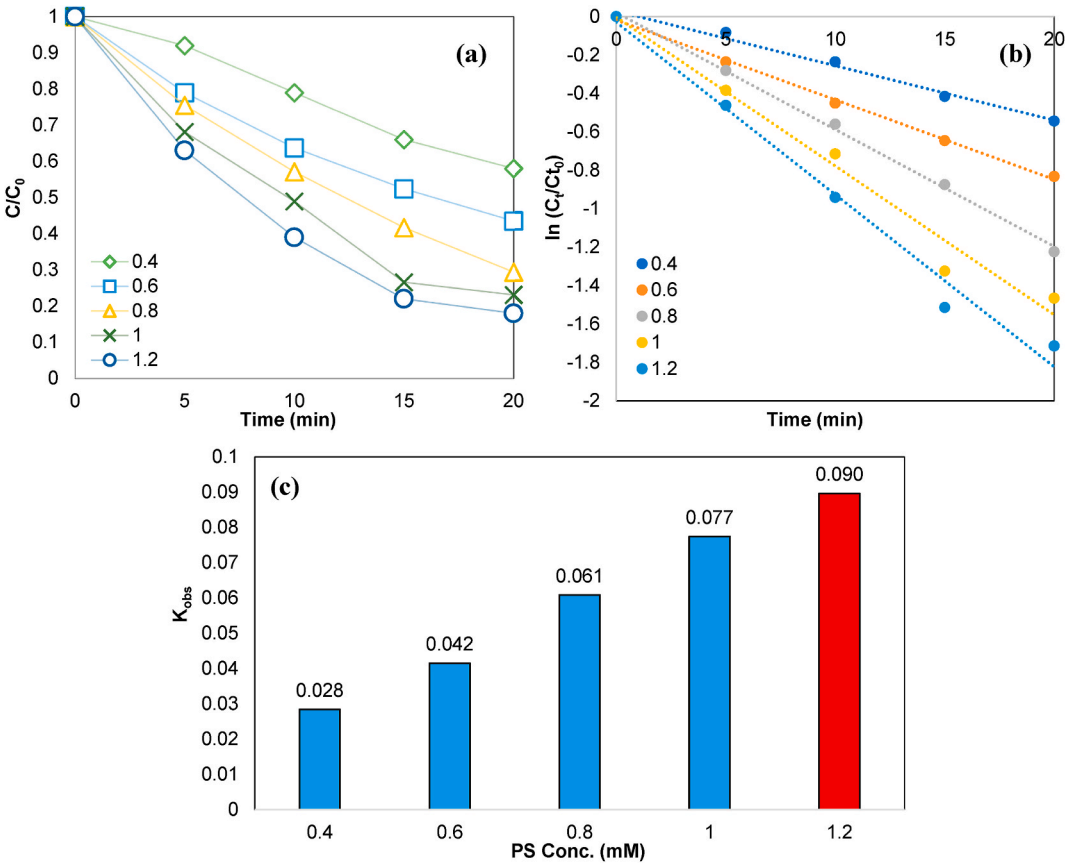

Fig. 5. Effect of PS concentration (mM) on furfural degradation (pH: 3, Catalysts dosage: 1 g/L, initial concentration: 20 mg/L, Volume: 200 mL) (a), kinetic study (b) and rate constant (c).

3.3.4. Effect of furfural concentration

The degradation of furfural by TZB nanocomposites was investigated at different furfural concentrations ranging from 10 to 45 mg/L. According to Fig. 6(a), at low concentrations (<10 mg/L), almost complete furfural removal was achieved within 15 min of the reaction. However, increasing the furfural concentration from 10 to 45 mg/L led to a decrease in the removal efficiency of TZB nanocomposites from almost 100 %–46 %. The reaction rate constant also decreased from 0.195 to 0.032 min^{-1} (Fig. 6(b-c)). This is likely due to the fact that increasing the furfural concentration leads to the saturation of active sites on the nano photocatalyst, making it less effective at degrading furfural. Consequently, $SO_4^{\circ-}$ and OH° radical generation is diminished [35]. Elevating the furfural concentration can reduce the number of photons reaching the nanophotocatalyst surface [36]. This phenomenon happens because UV light is absorbed by furfural molecules, reducing TZB nanophotocatalyst stimulation/excitation by photons.

3.4. Quenching agents

To ascertain the primary radical species in the PS/Catalysts/UV system, quenching experiments were executed under optimized conditions Four distinct radical scavengers including methanol, benzoquinone, potassium iodide, and *tert*-Butyl alcohol were applied at concentrations of 400 mM to quench the $SO_4^{\circ-}$, $O_2^{\circ-}$, H^+, and HO° radicals, respectively [37,38]. As depicted in Fig. 7, the introduction of methanol (MeOH) and *tert*-Butyl alcohol (TBA) led to a substantial reduction in degradation efficiency in comparison to potassium iodide (KI) and benzoquinone (BQ).

This observation implies that $SO_4^{\circ-}$ and OH° radicals hold greater significance in the degradation process. Furthermore, in terms of their impact on reduction efficiency, it is evident that methanol exerts a notably more potent inhibitory effect than *tert*-Butyl alcohol.

These outcomes validate that $SO_4^{\circ-}$ radicals take precedence as the primary radical species in the PS/Catalysts/UV system, emphasizing their prominent role in furfural degradation.

3.5. Degradation mechanism

The mechanism for furfural degradation using persulfate-assisted heterogeneous photocatalytic process by TiO_2–ZnO/biochar

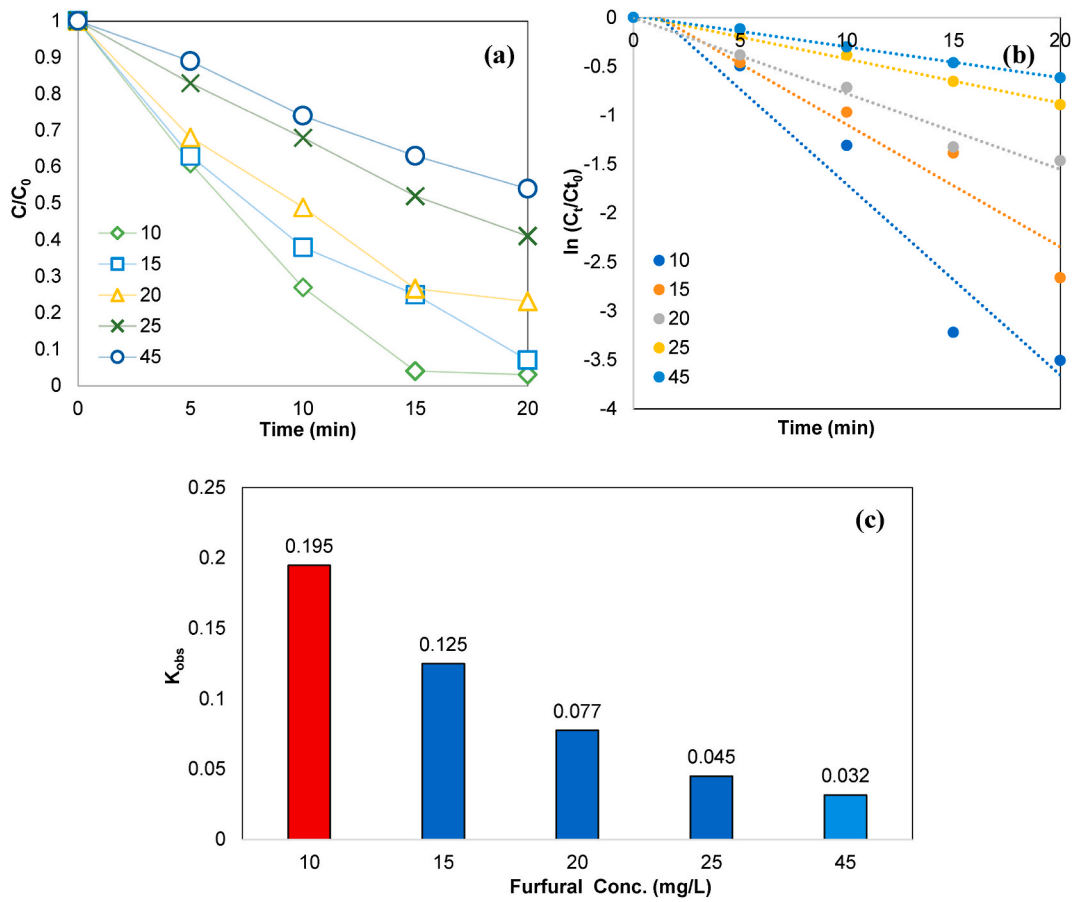

Fig. 6. Effect of initial concentration (mg/L) on furfural degradation (pH: 3, Catalyst dosage: 1 g/L, PS: 1.2 mM, Volume: 200 mL) (a), kinetic study (b) and rate constant (c).

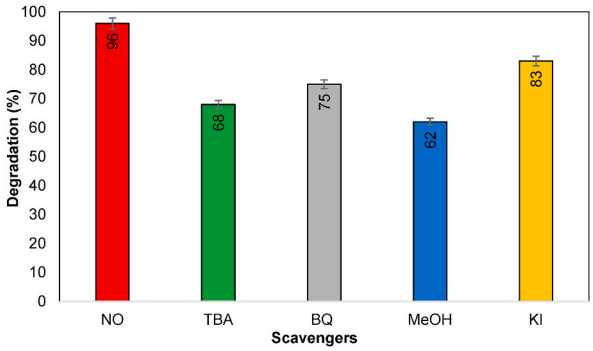

Fig. 7. Effect of various radical scavengers on furfural degradation (pH: 3, Catalyst dosage: 1 g/L, PS: 1.2 mM, Volume: 200 mL and, Time: 15min).

composite can be divided into the following steps.

I. Adsorption:

Furfural ($C_5H_4O_2$) + TiO_2–ZnO/biochar catalyst → Furfural adsorbed on the catalyst surface

II. Photocatalysis:

TiO_2–ZnO/biochar photocatalyst + UV light irradiation → Generation of electron-hole pairs, **Eqs. ((5), (6))**. These holes facilitate the oxidation of water molecules, resulting in the formation of hydroxyl radicals (OH°):

$$TiO_2\text{-}ZnO\,/\,biochar + UV \rightarrow e^- + h^+ \quad (5)$$

$$h^+ + H_2O \rightarrow OH^\circ + H^+ \quad (6)$$

III. Electron transfer:

e^- (from TiO_2–ZnO/biochar) + Persulfate ($S_2O_8^{2-}$) → reduce persulfate to sulfate radical anion ($SO_4^{\circ-}$), according to Eq. (7):

$$e^- + S_2O_8^{2-} \rightarrow SO_4^{\circ-} + SO_4^{2-} \quad \text{(eq. 7)}$$

IV. Radical reaction:

$SO_4^{\circ-}$ + Furfural adsorbed on the catalyst surface → Degradation of furfural and production of intermediates (Eq. (8)):

$SO_4^{\circ-}$ + $C_5H_4O_2$ → Furfural degradation + intermediates (e.g., 2-furoic acid ($C_5H_4O_4$), 2-furylaldehyde ($C_4H_4O_2$), and formic acid (CH_2O_2))(eq. 8)

V. Mineralization:

Continued degradation of furfural intermediates (presented in Eq. (9)) → Formation of simpler, less harmful end products (e.g., CO_2 and H_2O):

Furfural degradation intermediates + OH° + $SO_4^{\circ-}$ → CO_2 + H_2O (eq. 9)

In addition to the above steps, it is also important to consider the role of biochar in furfural degradation process. Biochar can play a number of roles in the process, including: (a) enhancing the photocatalytic activity of TiO_2–ZnO, (b) providing adsorption sites for furfural and other pollutants, and (c) generating reactive oxygen species (ROS) that can further degrade furfural.

4. Conclusion

Furfural represents a hazardous and enduring contaminant commonly encountered in industrial wastewater. It possesses the potential to infiltrate soil, water bodies, and even reach groundwater, leading to environmental contamination. Moreover, furfural is recognized as a carcinogenic agent and can cause various health effects. Consequently, the elimination of furfural from industrial wastewater is essential for protecting the environment and human health. Hereupon, the present study scrutinized the degradation of furfural, assessing the impact of pivotal parameters including pH, catalyst dosage, initial furfural concentration, and persulfate (PS) concentration, on the removal process and its associated kinetics. To achieve this objective, TiO_2–ZnO/biochar was fabricated via the

sol-gel technique and employed as a catalyst in the persulfate-assisted photocatalytic degradation of furfural. The findings demonstrated that, under the optimized conditions, a noteworthy 96 % of furfural was effectively eliminated, and the degradation process followed first-order kinetics. The degradation rate constant (Kobs) was further determined to be 0.195 min^{-1}. In the PS/Catalysts/UV system, it was established that both $SO4^{\circ-}$ and OH° radicals played crucial roles in furfural decomposition. Nevertheless, quenching experiments provided compelling evidence that $SO4^{\circ-}$ radicals exerted a more dominant influence in the degradation process. In summary, this investigation offers significant insights into the utility of TZB nanocomposites for furfural degradation and underscores the necessity of fine-tuning operational parameters to attain peak efficiency. The present study conspicuously showcased the commendable efficacy of TZB as a catalyst in the persulfate-assisted degradation process for furfural removal. These findings hold promise for the advancement of innovative and potent approaches to address furfural-contaminated industrial wastewater, thereby playing a pivotal role in environmental preservation and long-term sustainability.

Additional information

No additional information is available for this paper.

Data availability statement

Data will be made available on request.

CRediT authorship contribution statement

Maryam Hasanzadeh: Methodology. **Zeinab Ghaedrahmat:** Data curation, Methodology, Software. **Neda Kayedi:** Data curation, Methodology, Software. **Neamatollah Jaafarzadeh Haghighi Fard:** Conceptualization, Data curation, Formal analysis, Writing – original draft, Writing – review & editing. **Ali Azari:** Data curation, Formal analysis, Investigation, Methodology, Software, Writing – original draft, Writing – review & editing. **Maryam Afsharizadeh:** Data curation, Formal analysis, Investigation, Writing – original draft, Writing – review & editing.

Declaration of competing interest

The authors declare that they have no known competing financial interests or personal relationships that could have appeared to influence the work reported in this paper.

Acknowledgement

This study was financially supported by the Environmental Technologies Research Center, Ahvaz Jundishapur University of Medical Sciences, Ahvaz, Iran (Grant No. ETRC-9643 and Ethical code. IR. AJUMS.REC.1396.875).

References

[1] S. Uzoekwe, F. Oghosanine, The effect of refinery and petrochemical effluent on water quality of ubeji creek warri, southern Nigeria, Ethiopian Journal of Environmental Studies and Management 4 (2011) 107–116.
[2] A.A. Owodunni, S. Ismail, Revolutionary technique for sustainable plant-based green coagulants in industrial wastewater treatment—a review, J. Water Proc. Eng. 42 (2021), 102096.
[3] M.R. Samarghandi, M. Leili, K. Godini, J. Mehralipour, R. Harati, Furfural removal from synthetic wastewater by persulfate anion activated with electrical current: energy consumption and operating costs optimization, Der Pharma Chem. 7 (2015) 48–57.
[4] J.H. Arts, H. Muijser, M.J. Appel, C.F. Kuper, J.G. Bessems, R.A. Woutersen, Subacute (28-day) toxicity of furfural in Fischer 344 rats: a comparison of the oral and inhalation route, Food Chem. Toxicol. 42 (2004) 1389–1399.
[5] M. Wongkarnka, The Application of Aerobic Yeast for Treatment of High Strength Food Processing Wastewater Containing Furfural, Iowa State University, 2005.
[6] S. Ghosh, O. Falyouna, A. Malloum, A. Othmani, C. Bornman, H. Bedair, H. Onyeaka, Z.T. Al-Sharify, A.O. Jacob, T. Miri, A general review on the use of advance oxidation and adsorption processes for the removal of furfural from industrial effluents, Microporous Mesoporous Mater. (2021), 111638.
[7] A. Dargahi, M. Moradi, R. Marafat, M. Vosoughi, S.A. Mokhtari, K. Hasani, S.M. Asl, Applications of Advanced Oxidation Processes (Electro-Fenton and sono-electro-Fenton) for Degradation of Diazinon Insecticide from Aqueous Solutions: Optimization and Modeling Using RSM-CCD, Influencing Factors, Evaluation of Toxicity, and Degradation Pathway, Biomass Conversion and Biorefinery, 2021, pp. 1–18.
[8] S. Afshin, Y. Rashtbari, B. Ramavandi, M. Fazlzadeh, M. Vosoughi, S.A. Mokhtari, M. Shirmardi, R. Rehman, Magnetic nanocomposite of filamentous algae activated carbon for efficient elimination of cephalexin from aqueous media, Kor. J. Chem. Eng. 37 (2020) 80–92.
[9] G.P. Anipsitakis, D.D. Dionysiou, Transition metal/UV-based advanced oxidation technologies for water decontamination, Appl. Catal. B Environ. 54 (2004) 155–163.
[10] X. Ao, W. Liu, W. Sun, C. Yang, Z. Lu, C. Li, Mechanisms and toxicity evaluation of the degradation of sulfamethoxazole by MPUV/PMS process, Chemosphere 212 (2018) 365–375.
[11] J. Wang, S. Wang, Activation of persulfate (PS) and peroxymonosulfate (PMS) and application for the degradation of emerging contaminants, Chem. Eng. J. 334 (2018) 1502–1517.
[12] W. Wang, M. Chen, D. Wang, M. Yan, Z. Liu, Different activation methods in sulfate radical-based oxidation for organic pollutants degradation: catalytic mechanism and toxicity assessment of degradation intermediates, Sci. Total Environ. 772 (2021), 145522.
[13] T. Singh, N. Srivastava, P. Mishra, A. Bhatiya, N.L. Singh, Application of TiO2 nanoparticle in photocatalytic degradation of organic pollutants, in: Materials Science Forum, Trans Tech Publ, 2016, pp. 20–32.

[14] Z. Shayegan, C.-S. Lee, F. Haghighat, TiO2 photocatalyst for removal of volatile organic compounds in gas phase–A review, Chem. Eng. J. 334 (2018) 2408–2439.
[15] S.G. Kumar, L.G. Devi, Review on modified TiO2 photocatalysis under UV/visible light: selected results and related mechanisms on interfacial charge carrier transfer dynamics, J. Phys. Chem. 115 (2011) 13211–13241.
[16] M. Ni, M.K. Leung, D.Y. Leung, K. Sumathy, A review and recent developments in photocatalytic water-splitting using TiO2 for hydrogen production, Renew. Sustain. Energy Rev. 11 (2007) 401–425.
[17] M. Nasirian, Y. Lin, C. Bustillo-Lecompte, M. Mehrvar, Enhancement of photocatalytic activity of titanium dioxide using non-metal doping methods under visible light: a review, Int. J. Environ. Sci. Technol. 15 (2018) 2009–2032.
[18] S. Sargazi, E. Simge, S.S. Gelen, A. Rahdar, M. Bilal, R. Arshad, N. Ajalli, M.F.A. Khan, S. Pandey, Application of titanium dioxide nanoparticles in photothermal and photodynamic therapy of cancer: an updated and comprehensive review, J. Drug Deliv. Sci. Technol. (2022), 103605.
[19] M.E. Sümer, Enhanced Structural, Optical and Antibacterial Properties of ZnO Doped TiO2 composites/ZnO Katkılı TiO2 Kompozitlerin Geliştirilmiş Optik, Yapısal Ve Antibakteriyel Özellikleri, Kadir Has Üniversitesi, 2021.
[20] H. Sun, C. Kwan, A. Suvorova, H.M. Ang, M.O. Tadé, S. Wang, Catalytic oxidation of organic pollutants on pristine and surface nitrogen-modified carbon nanotubes with sulfate radicals, Appl. Catal. B Environ. 154 (2014) 134–141.
[21] Y. Shen, X. Ge, M. Chen, Catalytic oxidation of nitric oxide (NO) with carbonaceous materials, RSC Adv. 6 (2016) 8469–8482.
[22] C. Qin, H. Wang, X. Yuan, T. Xiong, J. Zhang, J. Zhang, Understanding structure-performance correlation of biochar materials in environmental remediation and electrochemical devices, Chem. Eng. J. 382 (2020), 122977.
[23] M. Vinayagam, S. Ramachandran, V. Ramya, A. Sivasamy, Photocatalytic degradation of orange G dye using ZnO/biomass activated carbon nanocomposite, J. Environ. Chem. Eng. 6 (2018) 3726–3734.
[24] R. Mohamed, A. Shawky, CNT supported Mn-doped ZnO nanoparticles: simple synthesis and improved photocatalytic activity for degradation of malachite green dye under visible light, Appl. Nanosci. 8 (2018) 1179–1188.
[25] X. Xie, S. Li, H. Zhang, Z. Wang, H. Huang, Promoting charge separation of biochar-based Zn-TiO2/pBC in the presence of ZnO for efficient sulfamethoxazole photodegradation under visible light irradiation, Sci. Total Environ. 659 (2019) 529–539.
[26] A. Peyghami, A. Moharrami, Y. Rashtbari, S. Afshin, M. Vosuoghi, A. Dargahi, Evaluation of the efficiency of magnetized clinoptilolite zeolite with Fe3O4 nanoparticles on the removal of basic violet 16 (BV16) dye from aqueous solutions, J. Dispersion Sci. Technol. 44 (2023) 278–287.
[27] H. Golestanifar, A. Asadi, A. Alinezhad, B. Haybati, M. Vosoughi, Isotherm and kinetic studies on the adsorption of nitrate onto nanoalumina and iron-modified pumice, Desalination Water Treat. 57 (2016) 5480–5487.
[28] X. Du, X. Bai, L. Xu, L. Yang, P. Jin, Visible-light activation of persulfate by TiO2/g-C3N4 photocatalyst toward efficient degradation of micropollutants, Chem. Eng. J. 384 (2020), 123245.
[29] W.-D. Oh, Z. Dong, T.-T. Lim, Generation of sulfate radical through heterogeneous catalysis for organic contaminants removal: current development, challenges and prospects, Appl. Catal. B Environ. 194 (2016) 169–201.
[30] J. Deng, C. Ye, A. Cai, L. Huai, S. Zhou, F. Dong, X. Li, X. Ma, S-doping α-Fe2O3 induced efficient electron-hole separation for enhanced persulfate activation toward carbamazepine oxidation: experimental and DFT study, Chem. Eng. J. 420 (2021), 129863.
[31] A. Rahmani, M. Salari, K. Tari, A. Shabanloo, N. Shabanloo, S. Bajalan, Enhanced degradation of furfural by heat-activated persulfate/nZVI-rGO oxidation system: degradation pathway and improving the biodegradability of oil refinery wastewater, J. Environ. Chem. Eng. 8 (2020), 104468.
[32] A.R. Rahmani, M. Salari, A. Shabanloo, N. Shabanloo, S. Bajalan, Y. Vaziri, Sono-catalytic activation of persulfate by nZVI-reduced graphene oxide for degradation of nonylphenol in aqueous solution: process optimization, synergistic effect and degradation pathway, J. Environ. Chem. Eng. 8 (2020), 104202.
[33] A. Shabanloo, M. Salari, N. Shabanloo, M.H. Dehghani, C.U. Pittman Jr., D. Mohan, Heterogeneous persulfate activation by nano-sized Mn3O4 to degrade furfural from wastewater, J. Mol. Liq. 298 (2020), 112088.
[34] A.D. Shiraz, A. Takdastan, S.M. Borghei, Photo-Fenton like degradation of catechol using persulfate activated by UV and ferrous ions: influencing operational parameters and feasibility studies, J. Mol. Liq. 249 (2018) 463–469.
[35] Z. Esmaili, A. Solaimany Nazar, M. Farhadian, Degradation of furfural in contaminated water by titanium and iron oxide nanophotocatalysts based on the natural zeolite (clinoptilolite), Sci. Iran. 24 (2017) 1221–1229.
[36] H.R. Rajabi, O. Khani, M. Shamsipur, V. Vatanpour, High-performance pure and Fe3+-ion doped ZnS quantum dots as green nanophotocatalysts for the removal of malachite green under UV-light irradiation, J. Hazard Mater. 250 (2013) 370–378.
[37] Y. Feng, C. Liu, J. Chen, H. Che, L. Xiao, W. Gu, W.J.R.A. Shi, Facile synthesis of BiOI/CdWO 4 p–n junctions, enhanced photocatalytic activities and photoelectrochemistry 6 (2016) 38290–38299.
[38] H. Wang, J. Deng, X. Lu, L. Wan, J. Huang, Y. Liu, Rapid and continuous degradation of diclofenac by Fe (II)-activated persulfate combined with bisulfite, Separ. Purif. Technol. 262 (2021), 118335.